

# MULTI-SPECTRAL VISION PROCESSING FOR THE EXOMARS 2018 MISSION

Dave Barnes<sup>1</sup>, Martin Wilding<sup>1</sup>, Matt Gunn<sup>1</sup>, Stephen Pugh<sup>1</sup>, Laurence Tyler<sup>1</sup>, Andrew Coates<sup>2</sup>, Andrew Griffiths<sup>2</sup>, Claire Cousins<sup>3</sup>, Nicole Schmitz<sup>4</sup>, Arnold Bauer<sup>5</sup>, and Gerhard Paar<sup>5</sup>

<sup>1</sup>*Aberystwyth University\*, SY23 3DB, UK*

<sup>2</sup>*MSSL, University College London, RH5 6NT, UK*

<sup>3</sup>*Centre for Planetary Sciences, University College London, WC1E 6BT, UK*

<sup>4</sup>*DLR, Institute of Planetary Research, Rutherfordstrasse 2, 12489, Berlin, Germany*

<sup>5</sup>*Joanneum Research, Steyrergasse 17, A-8010, Graz, Austria*

## ABSTRACT

Radiometric calibration is a key activity being undertaken for the science cameras which are part of the Panoramic Camera (PanCam) instrument for the ESA/NASA 2018 ExoMars mission. The PanCam instrument is designed to be the ‘eyes’ of the Mars rover and is equipped with two wide angle multi-spectral cameras (WACs) from MSSL, and a focusable High Resolution Camera (HRC) from DLR. To achieve its science role within the ExoMars mission, the PanCam must be able to generate terrain reflectance spectra to help identify the mineralogy of the Martian surface, and able to generate true-colour images of the Martian environment. These images will be scrutinised by scientists back on Earth for possible exobiology clues. Aberystwyth University (AU) is responsible for delivering the PanCam Calibration Target (PCT) which is an essential component for the science operations of the PanCam instrument. Its purpose is to allow radiometric calibration and to support geometric calibration check-out of the PanCam instrument during the ExoMars mission. Unlike other camera calibration targets flown to Mars, the PCT target regions are being made from stained glass. The paper describes the work undertaken during the design, early build and testing of the PCT, together with results from the baseline algorithms that have been designed and implemented to process the multi-spectral PanCam images.

Key words: ExoMars 2018; PanCam; radiometric; colourimetric; multi-spectral; calibration target.

## 1. INTRODUCTION

The ESA ExoMars 2018 rover [1] supports many science instruments dedicated to the exploration of Mars and the search for past or present life. The rover has a mast with a pan and tilt unit which interfaces to the Panoramic Camera (PanCam) instrument. The purpose of the PanCam [5]



Figure 1. EADS Astrium Bridget rover with the AU PanCam Emulator (AUPE) undergoing field trial experiments at Clarach Bay beach, Ceredigion, UK.

instrument which is led by MSSL is to provide images of the rover and its surroundings and support the movement of the rover over the Martian terrain; to investigate the geology of Martian terrain; to study the atmosphere, and support the other ExoMars instruments in the search for evidence of life on Mars. The PanCam comprises two wide angle multi-spectral cameras (WACs) each with 12 filters and a Field Of View (FOV)  $\approx 34^\circ$ , and a High Resolution Camera (HRC) with a FOV  $\approx 5^\circ$ .

The Martian surface is subjected to very high levels of UV irradiation which fades colours over time and therefore alters the radiometric properties of a calibration target. We know from the stained glass windows found in medieval churches that coloured glass is very UV tolerant, hence we have decided to use stained glass as the basis for the greyscale and colour targets required for the ExoMars 2018 PanCam Calibration Target (PCT).

So that science target spectra can be generated (e.g. for rock mineralogy) the returned WAC images will be radiometrically corrected. Using pre-flight PCT data, this correction will partially remove the radiometric effects of the Martian sky upon the science targets under investigation.

\*Corresponding Author: Prof. Dave Barnes, email: [dpb@aber.ac.uk](mailto:dpb@aber.ac.uk)

All science target spectra generated during the mission will be referenced to certified standards and thus allow both Mars and terrestrial generated spectra comparison. Additionally, the radiometrically corrected filtered images for those wavelengths within the human visible light region will be used to create 'true-colour' image products of the Martian surface. We have designed and implemented a baseline radiometric and colourimetric processing pipeline capable of performing the required radiometric correction and generating true-colour image products.

Testing of the prototype PCT and baseline radiometric and colourimetric processing pipeline software has involved a number of field trials near Aberystwyth (Fig. 1), and during the AMASE Arctic Mars Analogue Svalbard Expedition. This paper provides an overview of our current prototype PCT design together with details of our baseline radiometric and colourimetric processing algorithm, and presents results from our field trial tests.

## 2. PANCAM CALIBRATION TARGET (PCT)

There have been a number of camera calibration targets used on Mars during the Viking Landers mission (1976), the Mars Pathfinder mission with the Sojourner rover (1997), the two Mars Exploration Rovers (MER), Spirit and Opportunity (2004), and the Phoenix Lander Mars mission (2008). All of these missions have flown multi-spectral cameras and have required a camera calibration target within sight of the imaging system to be able to perform image radiometric correction, and to generate true-colour image products. Each of the Viking Landers [10] had three colour/contrast/sharpness test charts that were mounted approximately  $35^\circ$  degrees from the vertical within the field of view (FOV) of the two facsimile-type cameras. The Mars Pathfinder mission saw the introduction of a new design of calibration target. The lander had two calibration targets [11], one above most of the spacecraft and the other at the extreme of the spacecraft base plate. Each target had greyscale and colour regions mounted within the horizontal plane. The greyscale regions were composed of concentric circles with a shadow post mounted vertically at the centre. This design was enhanced for the MER mission [4] resulting in the iconic MER 'sundial' design. Again concentric greyscale regions with a single shadow post were used, and four colour regions were introduced at the corners. A space qualified polymer (GE RTV 655) was used which was impregnated with inorganic pigment material (e.g. metal oxides) to produce the four colours. For the Phoenix Lander the calibration target design was further enhanced by the introduction of sweep magnets [7] situated beneath the greyscale and colour targets. The presence of the magnets served to keep the central region of the targets as clean of magnetic dust as possible. As the UV irradiation on the Martian surface can alter the optical properties of reflecting materials, the colour targets were artificially aged by exposure to UV irradiation. This was equivalent to two months of exposure on the Martian surface, thus minimising any further changes during the mission.

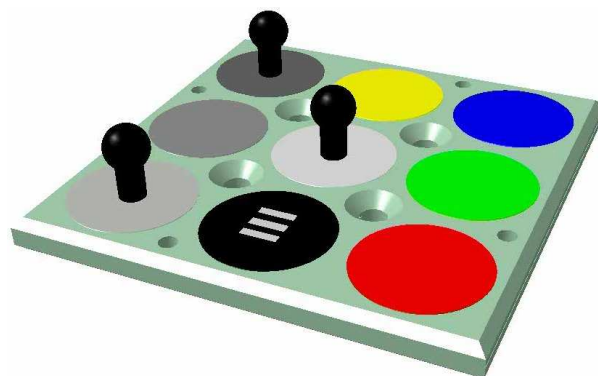


Figure 2. PanCam Calibration Target (PCT) CAD model.

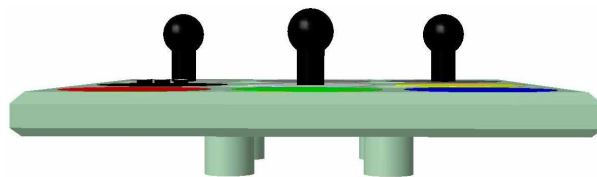


Figure 3. Side view of PCT model showing the PCT mounting pads.

The significant contribution of Dan Britt from the University of Central Florida to the field of radiometric calibration targets should be noted. He has been responsible for the development and build of the radiometric calibration targets for Mars Pathfinder, MER, Mars Polar Lander, Mars Phoenix, and the MER flight spare (FS) calibration target which will fly on the Mars Science Laboratory (MSL) mission (launch 2011).

Whilst we have learnt a great deal from the design of the radiometric calibration targets flown on previous missions, we wished to develop our own approach to the problems faced by such targets. Accordingly we have designed our own radiometric calibration target which draws upon certain elements of the previously flown targets. Nevertheless, we have our own distinctive design.

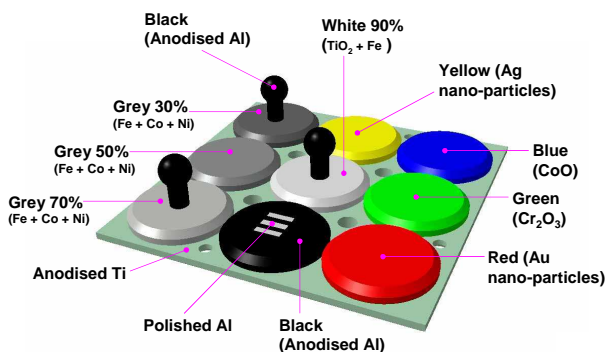


Figure 4. PCT stained glass chemistry. The top retaining plate has been removed. Note that the glass wafers have a reflective back coating.

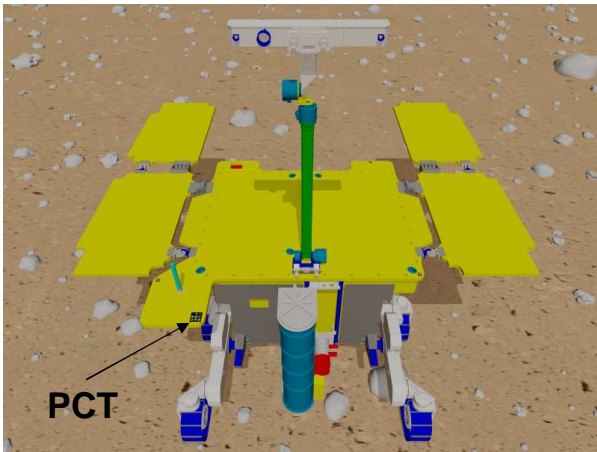


Figure 5. ExoMars 2018 PCT accommodation (TBC).

The current PCT design is 50 mm × 50 mm, 16 mm in height, and has a mass budget of 20 gm + 20% contingency. Fig. 2 and Fig. 3 show the current CAD model for the PCT which is composed of mounting pads, a base plate, a layer of calibration targets, a top retaining plate and three shadow posts. Fig. 5 shows the proposed accommodation (to be confirmed - TBC) of the PCT on the ExoMars rover top deck.

To ensure that the radiometric properties of the PCT don't change during the mission due to the high UV irradiation whilst on the Martian surface, we have decided to use annealed stained glass for our greyscale and colour targets. Fig. 4 shows an overview of the chemistry needed to create the required greys and colours. The base and retaining plates are made from (anodised) Titanium (colour TBC) which has a coefficient of thermal expansion close to that of glass. The glass targets are soda-lime-silica based to which small quantities of Cerium are added to radiation harden the glass. The addition of appropriate metals or metal oxides to the glass mix prior to heating produces the variety of greyscale (90%, 70%, 50% and 30% reflectance) and colour glasses (red, green, blue and yellow). We use a core drill to remove a cylinder of stained glass from the quenched glass mix, and the core is then sectioned into stained glass wafers. Each wafer is given a reflective Aluminium back coating to increase the amount of reflected light. We are currently investigating the top surface treatment for the stained glass wafers. Ideally they need to have a Lambertian reflectance property, but not act as a trap for the fine Martian dust particles. The 'white' glass wafer is slightly greyed and the black wafer is made from anodised Aluminium. The top surface of the black wafer has three raised 'bars' each with a polished top surface to provide a high contrast against the black background. These bars act as calibration targets for the HRC focus mechanism during surface operations.

Rather than use a single central shadow post and concentric greyscale regions, we have opted to use three shorter shadow posts each centred upon separate greyscale glass wafers. The shadow posts allow terrain regions in a captured image that are illuminated only by diffuse sky illu-



Figure 6. An earlier version of the PCT top retaining plate (inverted) with example stained glass wafers.

mination (as opposed to direct sunlight) to be sampled. The use of a single short shadow post for each grey wafer minimises the need to compensate for shadow density changes observed when a taller post is used, and the radial distance from the post increases as the shadow falls across the concentric greyscale regions [13].

The use of Titanium, Aluminium and stained glass is important from the standpoint of planetary protection (PP) as the surfaces can be cleaned with isopropyl alcohol (IPA) to reduce bio-burden, and withstand the process of Dry Heat Microbial Reduction (DHMR) (e.g. 125°C for 30 hrs).

Fig. 6 shows prototype example greyscale and colour stained glass wafers and we have undertaken their preliminary characterisation (see Fig. 7). Whilst there is room for improvement (e.g. colour homogeneity) in our stained glass composition and manufacturing process, the data are encouraging.

For the characterisation process in addition to spectrometers, NIST traceable calibrated reflectance standards, integrating spheres, and a NIST traceable calibrated uniform light source, we have a gonireflectometer. This permits measurement of the bidirectional reflectance distribution functions (BRDF), and bidirectional surface scattering distribution functions (BSSRDF) for each of the PCT greyscale and colour wafers.

### 3. RADIOMETRIC AND COLOURIMETRIC PROCESSING PIPELINE

To test our PCT design required us to develop and implement a software-based radiometric and colourimetric

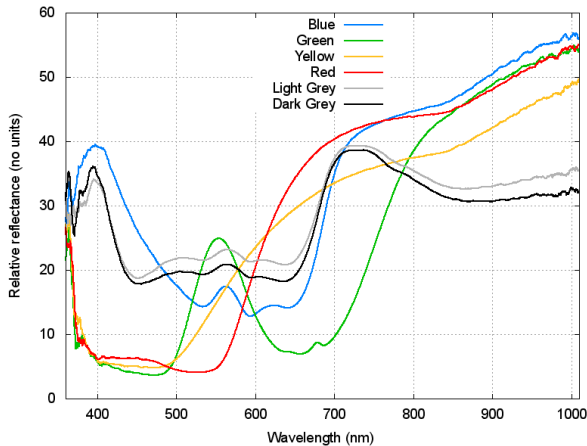


Figure 7. Graph of the measured relative reflectance values for each of the prototype PCT stained glass wafers.

image processing pipe-line. Given the previous multi-spectral cameras flown to Mars, a good deal of research has been conducted in the area of processing multi-spectral image data to generate terrain Region of Interest (ROI) reflectance spectra, and colour corrected products. This work includes for example, the Viking Lander Mission [6], Mars Pathfinder [9], [11], MER [2], [3], and Phoenix [8].

We have developed our own algorithms based upon this previous work, and Fig. 8 shows a generalised overview of our current radiometric and colourimetric image processing pipeline. It should be noted that Fig. 8 does not show all of the processing stages that will be required for the ExoMars 2018 mission. Rather it represents a baseline that has allowed us to conduct performance evaluation experiments with our current PCT design. The eventual image processing pipeline for the ExoMars 2018 mission will be a complete and enhanced version based upon this early processing pipeline work.

During the ExoMars 2018 mission PanCam WAC multi-spectral images of the surrounding Martian environment and the PCT will be captured. Ideally the images of the PCT will be captured within the same time frame, and hence the lighting conditions will be similar for all of the images. The Martian environment and PCT images will be compressed for downlink to Earth. We have assumed lossless compression for the tests that we have performed to date, but we will need to revisit this area in the future as a variety of compression strategies will be used during the mission. All downlinked data will be stored on the ESA PDS using the NASA Planetary Data System (PDS) standard. Once uncompressed the downlinked images can be processed using the radiometric and colourimetric processing pipeline. An overview of the subsequent stages is presented in sections 3.1 to 3.5.

### 3.1. Camera Radiometric Correction

The PanCam WAC images downlinked from Mars will contain raw Data Number (DN) values for each pixel. The purpose of the camera radiometric correction process is to convert these raw DN values into calibrated radiance units for each filter wavelength ( $W \cdot sr^{-1} \cdot m^{-2} \cdot nm^{-1}$ ). Thus effectively converting the PanCam WACs into absolute spectroradiometer instruments from which terrain ROI reflectance spectra, and true-colour image products can be obtained. A sequence of corrections are required involving activities such as PanCam WAC detector bias subtraction, dark frame subtraction and flat-fielding. The data used during these stages need to be referenced to appropriate operational parameters such as camera temperature and exposure time during image capture. We also need to perform a camera detector radiometric response correction to complete the DN to spectral radiance conversion. We have used our laboratory radiometric characterisation equipment (integrating spheres, calibrated uniform light source etc.) to measure the CCD radiometric response function of our field trial camera system (see Fig. 9), and to capture darks, and flat-field frames, and made a number of calibrated flat field images which we have used during this part of the processing pipeline. It should be noted that prior to launch a comprehensive PanCam radiometric calibration campaign will be conducted to capture all of the required camera(s) radiometric correction data.

### 3.2. Relative Reflectance - $R^*$

The next stage in the processing pipeline involves converting each radiometrically corrected filter image into  $R^*$  (“R-star”) data.  $R^*$  was defined by [11] as “the brightness of the surface divided by the brightness of an RT (Radiometric Calibration Target) scaled to its equivalent Lambert reflectance.” Reference [2] notes that “ $R^*$  is useful in that it allows for direct comparison between spectra taken at different times of day, and more straightforward comparison with laboratory spectra.”

Our current processing pipeline generates  $R^*$  data for each filtered image ( $R_{\lambda}^*$ ) using Eq. 1 where  $\lambda$  denotes the filter used.

$$R_{\lambda}^* = (RC_{\lambda} \cdot m_{\lambda}) \cdot e_{\lambda}^{-1} \quad (1)$$

$RC_{\lambda}$  is a radiometrically corrected image from the previous stage,  $e_{\lambda}$  is the image exposure value, and  $m_{\lambda}$  is the slope of the straight line fit between the observed image PCT reflectance values on Mars, and those PCT reflectance values measured during the pre-flight laboratory characterisation activity. Prior to launch the BRDF of each of the PCT greyscale and colour targets will be measured for each PanCam WAC filter wavelength. Provided we know the Sun’s azimuth and elevation when an image is captured on Mars, we can process the BRDF data to determine the laboratory reflectance values for each of the

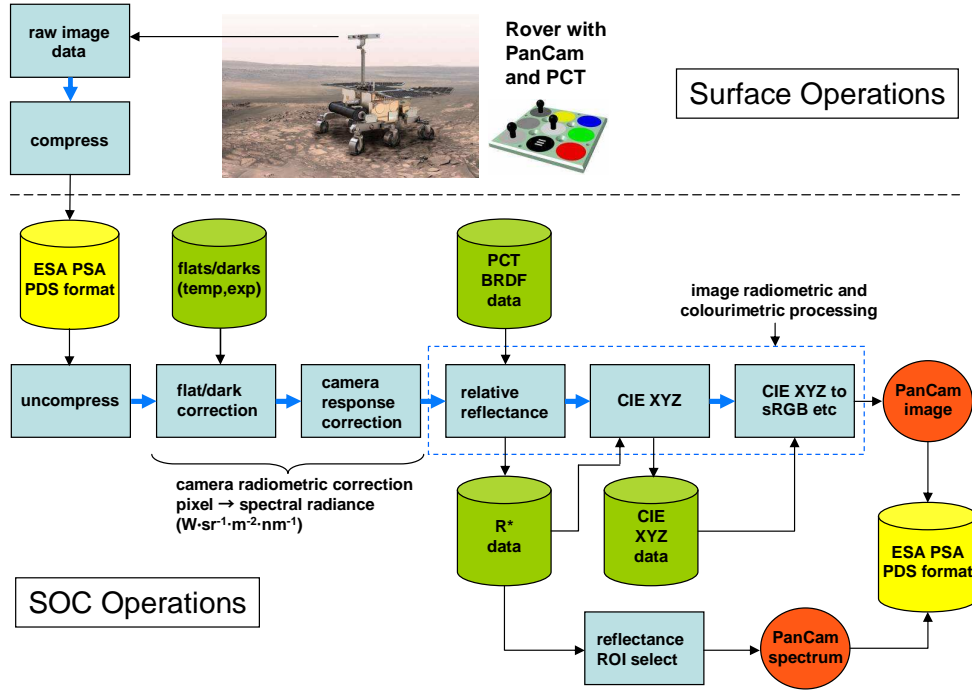


Figure 8. Generalised radiometric and colourimetric processing pipeline being developed for the ExoMars 2018 Science Operations Centre (SOC). Note the pipeline is under development and the schematic above represents our current baseline implementation for the purpose of conducting preliminary tests on our PCT design. The details of the interface to the ESA Planetary Science Archive (PDS) are not shown, and have been generalised.

PCT targets. For the filtered images of the PCT downlinked from Mars, the PCT targets will be sampled and the mean, median, standard deviation and variance calculated. These ‘on Mars’ data points can be plotted against the laboratory measured data points and a straight line fitted to determine  $m_\lambda$ . Currently we use either an ordinary least squares (OLS) fitting algorithm, or a weighted least squares (WLS) algorithm where the weights for the ‘on Mars’ data points are inversely proportional to their variance.

### 3.3. Region Of Interest (ROI) Reflectance Spectra

Once  $R^*$  data have been generated from a downlinked filter image set of a particular scene on Mars, then reflectance spectra can be generated. This process involves identifying a ROI in one of the returned images (e.g. a rock surface pixel area) and extracting this ROI data from each of the  $R_\lambda^*$  data files. Currently we determine the mean and standard deviation for each  $R_\lambda^*$  ROI, and fit a straight line between each data point. As the current PanCam WAC design has geology filters distributed between both left and right WACs, then a ROI in a left-hand image, for example, has to be identified in the right-hand image. The plotted reflectance spectra can be used to identify the mineralogy of the ROI under investigation.

### 3.4. Generating CIE XYZ Data

Using the International Commission on Illumination (CIE) standardised method for the reflective (or transmissive) case, the CIE tristimulus values ( $XYZ$ ) can be obtained by multiplying the object (pixel) reflectance spectrum  $R(\lambda)$ , the relative spectral power of the illuminant  $S(\lambda)$  and each of the colour matching functions of the 1931 CIE standard observer,  $\bar{x}(\lambda)$ ,  $\bar{y}(\lambda)$ ,  $\bar{z}(\lambda)$  (Eq. 2). Common CIE standardised illuminants include  $D_{50}$  and  $D_{65}$ .

$$\begin{aligned} X &= K \int_0^\infty R(\lambda)S(\lambda)\bar{x}(\lambda) d\lambda \\ Y &= K \int_0^\infty R(\lambda)S(\lambda)\bar{y}(\lambda) d\lambda \\ Z &= K \int_0^\infty R(\lambda)S(\lambda)\bar{z}(\lambda) d\lambda \end{aligned} \quad (2)$$

$K$  is a normalisation constant and is chosen to give  $Y = 100$  for the case of a perfect white Lambertian reflector ( $R(\lambda) = 1$ ) i.e. when an object (pixel) reflects 100% for all wavelengths (Eq. 3).

$$K = \frac{100}{\int_0^\infty S(\lambda)\bar{y}(\lambda) d\lambda} \quad (3)$$

One method of computing the CIE tristimulus values is to first fit a cubic spline function to each ‘pixel’ across a given  $R_\lambda^*$  data set, e.g. within the spectral range  $360\text{nm} \leq \lambda \leq 830\text{ nm}$ . Each pixel cubic spline function, i.e.  $R(\lambda)$ , interpolated at 1 nm resolution can then be summed over the range of  $\lambda$  with the appropriate  $S(\lambda)$  function, and corresponding  $\bar{x}(\lambda)$ ,  $\bar{y}(\lambda)$ , or  $\bar{z}(\lambda)$  function also at 1 nm resolution.

To normalise the calculated tristimulus values and thus define the resultant image luminance (brightness), we sample the PCT white target region in the  $R_\lambda^*$  data set being used, calculate the CIE  $Y$  value for each pixel in the sample, and then determine the mean of these CIE  $Y$  values to produce a value  $N$ . Each CIE  $XYZ$  value is then multiplied by  $1/N$ .

If required the CIE chromaticity coordinates for an object (pixel) can be calculated by normalising the tristimulus values (Eq. 4).

$$\begin{aligned} x &= X/(X + Y + Z) \\ y &= Y/(X + Y + Z) \\ z &= Z/(X + Y + Z) \end{aligned} \quad (4)$$

### 3.5. Converting CIE XYZ Data to sRGB

The final stage in the processing pipeline is to convert the device independent CIE  $XYZ$  values to sRGB data for example, so that the resultant colour corrected image can be displayed on a computer monitor, or printer. The transformation process from 1931 CIE  $XYZ$  values to sRGB has been defined by the International Electrotechnical Commission (IEC) [12]. In the case of sRGB the colour space reference white is defined relative to the CIE  $D_{65}$  illuminant (i.e.  $x = 0.3127$ ,  $y = 0.3290$ ,  $z = 0.3583$ ), and a standard transformation matrix can be applied to the CIE  $XYZ$  tristimulus values (Eq. 5).

$$\begin{bmatrix} r \\ g \\ b \end{bmatrix} = [M] \begin{bmatrix} X \\ Y \\ Z \end{bmatrix} \quad (5)$$

where

$$[M] = \begin{bmatrix} 3.2404542 & -1.5371385 & -0.4985314 \\ -0.9692660 & 1.8760108 & 0.0415560 \\ 0.0556434 & -0.2040259 & 1.0572252 \end{bmatrix}.$$

Once the CIE  $XYZ$  tristimulus values are converted to linear  $r, g, b$ , the resultant data can be clipped to lie within the range of 0 to 1 (Eq. 6). The subsequent stage is to apply a gamma correction so that the final sRGB image data will display correctly on a (generic) computer monitor (Eq. 7).

$$\alpha = \begin{cases} 1 & \beta > 1 \\ 0 & \beta < 0 \\ \beta & \text{otherwise} \end{cases} \quad (6)$$

where  $\alpha \in \{r_c, g_c, b_c\}$  and  $\beta \in \{r, g, b\}$ .

$$\gamma = \begin{cases} 12.92\alpha & \alpha \leq 0.0031308 \\ 1.055(\alpha)^{1/2.4} - 0.055 & \alpha > 0.0031308 \end{cases} \quad (7)$$

where  $\gamma \in \{r_\gamma, g_\gamma, b_\gamma\}$ .

The resultant gamma corrected values  $r_\gamma, g_\gamma, b_\gamma$  are in the range of 0 to 1, and hence they can be scaled and rounded to the nearest integer to yield the final sRGB format image data (Eq. 8).

$$d = \text{round}(((W_{DC} - B_{DC}) \times \gamma) + B_{DC}) \quad (8)$$

where  $d \in \{sR, sG, sB\}$ ,  $W_{DC}$  = the white digital count, e.g. 255 for 8-bit data products, and  $B_{DC}$  = the black digital count, e.g. 0.

## 4. PCT FIELD TRIALS

To test our current PCT design we have captured images of a prototype PCT during field trials at Clarach Bay beach, Ceredigion, UK. PanCam colleagues from DLR, MSSL, and Joanneum Research have also undertaken trials as part of the Artic Mars Analog Svalbard Expedition (AMASE). The AU (multi-spectral) PanCam Emulator (AUPE) has been used for the field trials, Fig. 9. The AUPE uses COTS monochromatic cameras with optics and filters that approximate to the PanCam instrument design. Each AUPE ‘WAC’ has a motorised filter wheel with 9 filters, Tab. 1. Currently we use the broadband (100 nm) filters to generate a quick look colour image, and use the narrowband (10 nm) filters when capturing images to be processed by our baseline radiometric and colourimetric pipeline software. The baseline algorithms have been implemented in Mathcad and ported to both Java and LabVIEW.

Fig. 10 shows AMASE AUPE WAC captured data that have been processed to generate reflectance spectra of various science targets (ROI) identified within the captured image data. Images captured using the (10 nm) filters on both the left and right AUPE WACs were used as the input data. We had a simple PCT prototype during these trials, yet despite its simplicity we were able to generate ROI reflectance spectra. We did observe incorrect reflectance data being generated when using the 950 nm filter, but this was due to interference fringes

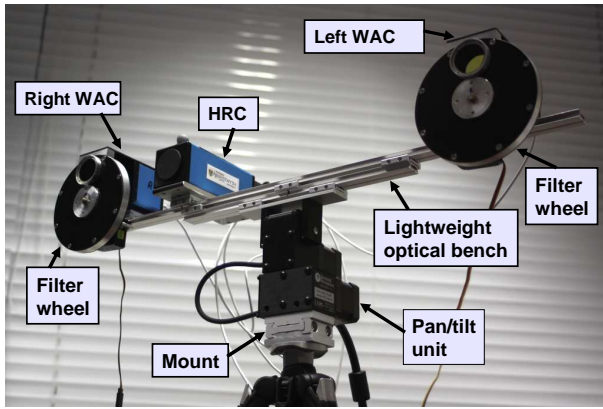


Figure 9. The AU (multi-spectral) PanCam Emulator (AUPE).

Table 1. AU PanCam Emulator (AUPE) Filter Data

Left Filter Wheel	Centre (nm)	Width (nm)
Blue	460	≈ 100
Green	550	≈ 100
Red	660	≈ 100
Geol1	440	10
Geol2	470	10
Geol3	510	10
Geol4	560	10
Geol5	600	10
Geol6	660	10
Right Filter Wheel	Centre (nm)	Width (nm)
Blue	460	≈ 100
Green	550	≈ 100
Red	660	≈ 100
Geol7	720	10
Geol8	760	10
Geol9	830	10
Geol10	880	10
Geol11	950	10
Geol12	1000	10

within our filter wheel, and not our simple PCT, or processing pipeline. We need to reduce the larger standard deviations that we are experiencing for some of the data points, and we believe that a more detailed camera calibration campaign will resolve this problem.

Fig. 11 and Fig. 12, show true-colour corrected images generated from AMASE and Clarach Bay data. For each case the (10 nm) filters on the left AUPE WAC were used. For the Clarach Bay trials we introduced a Gretag Macbeth ColorChecker which we can use to compare the generated colours against laboratory measured data. Currently we are implementing colour difference measurement methods so that we can quantify the colour correctness of our baseline colourimetric processing algorithms. We are investigating different methods for generating CIE  $XYZ$  data, and it is important to know if different algorithms result in perceptible colour changes.

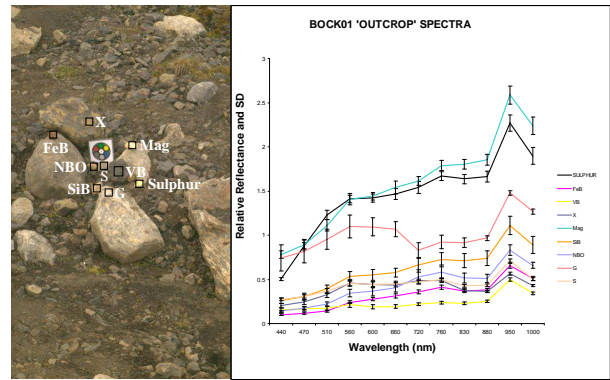


Figure 10. Example of relative reflectance spectra results from the AMASE field trials.

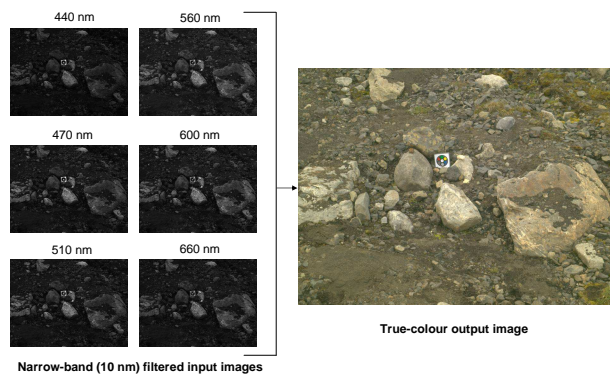


Figure 11. Example of colour correction results from the AMASE field trials.

## 5. CONCLUSION

The paper has reported on our current design work for the ExoMars 2018 PanCam Calibration Target (PCT). We have used a stained glass approach that will overcome the problem of high UV irradiation and colour 'fade' during the mission. Our design is well suited to the demands of PP, and glass has the attraction that a large number of surface treatments are available to reduce possible issues such as specular reflection. We have been encouraged by the preliminary radiometric characterisation of our early stained glass wafers. We have presented a baseline radiometric and colourimetric image processing pipeline that has been designed for the purpose of testing our PCT. Our algorithms have been implemented in software and we have conducted a number of field trials where multi-spectral images of a PCT prototype have been captured. The generated reflectance spectra and colour corrected image results are encouraging. Future complete and enhanced versions of our radiometric and colourimetric image processing pipeline will be used during the ExoMars 2018 mission.

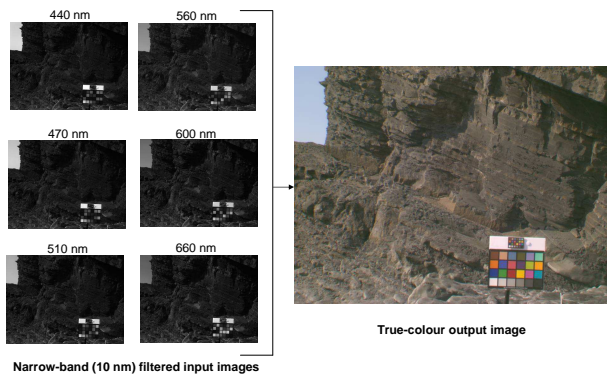


Figure 12. Example of colour correction results from the Clarach Bay field trials.

## ACKNOWLEDGMENTS

The research leading to these results has been funded by the UK Space Agency, Grant No. ST/G003114/1, and Grant No. ST/I002758/1, together with contributions from The European Community's Seventh Framework Programme (FP7/2007-2013), Grant Agreement No. 218814 PRoVisG, and Grant Agreement No. 241523 PRoVisScout.

## REFERENCES

- [1] D. Barnes, E. Battistelli, R. Bertrand, F. Butera, et al., and the Rover Team. The ExoMars rover and Pasteur payload Phase A study: an approach to experimental astrobiology. *International Journal of Astrobiology*, 5:221–241, 2006.
- [2] J. Bell, J. Joseph, J. Sohl-Dickstein, H. Arneson, M. Johnson, M. Lemmon, and D. Savransky. In-flight calibration and performance of the Mars Exploration Rover Panoramic Camera (Pancam) instruments. *Journal of Geophysical Research-Planets*, 111(E2), Jan. 6 2006.
- [3] J. Bell, D. Savransky, and M. J. Wolff. Chromaticity of the Martian sky as observed by the Mars Exploration Rover Pancam instruments. *Journal of Geophysical Research-Planets*, 111(E12), Sep. 28 2006.
- [4] J. Bell, S. Squyres, K. Herkenhoff, J. Maki, H. Arneson, D. Brown, S. Collins, A. Dingizian, S. Elliot, E. Hagerott, A. Hayes, M. Johnson, J. Johnson, J. Joseph, K. Kinch, M. Lemmon, R. Morris, L. Scherr, M. Schwochert, M. Shepard, G. Smith, J. Sohl-Dickstein, R. Sullivan, W. Sullivan, and M. Wadsworth. Mars Exploration Rover Athena Panoramic Camera (Pancam) investigation. *Journal of Geophysical Research-Planets*, 108(E12), Nov. 29 2003.
- [5] A. D. Griffiths, A. J. Coates, R. Jaumann, H. Michaelis, G. Paar, D. Barnes, J.-L. Josset, and the PanCam Team. Context for the ESA ExoMars rover: the Panoramic Camera PanCam instrument. *International Journal of Astrobiology*, 5:269–275, 2006.
- [6] F. O. Huck, D. J. Jobson, S. K. Park, S. D. Wall, R. E. Arvidson, W. R. Patterson, and W. D. Benton. Spectrophotometric and color estimates of the Viking lander sites. *Journal of Geophysical Research*, 82:4401–4411, Sept. 1977.
- [7] K. Leer, P. Bertelsen, C. S. Binau, L. D. Olsen, L. Drube, T. V. Falkenberg, M. P. Haspang, M. B. Madsen, M. Olsen, H. Sykulska, S. Vijendran, W. T. Pike, U. Staufer, D. Parrat, M. Lemmon, M. H. Hecht, C. T. Mogensen, M. A. Gross, W. Goetz, J. Marshall, D. Britt, P. Smith, C. Shinohara, P. Woida, R. Woida, R. Tanner, R. Reynolds, and A. Shaw. Magnetic properties experiments and the Surface Stereo Imager calibration target onboard the Mars Phoenix 2007 Lander: Design, calibration, and science goals. *Journal of Geophysical Research-Planets*, 113, Oct. 7 2008.
- [8] M. T. Lemmon, P. H. Smith, C. Shinohara, R. Tanner, P. Woida, A. Shaw, J. Hughes, R. Reynolds, R. Woida, J. Penegor, C. Oquest, S. F. Hviid, M. B. Madsen, M. Olsen, K. Leer, L. Drube, R. V. Morris, and D. T. Britt. The Phoenix Surface Stereo Imager (SSI) Investigation. In *Lunar and Planetary Institute Science Conference Abstracts*, volume 39 of *Lunar and Planetary Inst. Technical Report*, pages 2156–+, Mar. 2008.
- [9] J. Maki, J. Lorre, P. Smith, R. Brandt, and D. Steinwand. The color of Mars: Spectrophotometric measurements at the Pathfinder landing site. *Journal of Geophysical Research-Planets*, 104(E4):8781–8794, Apr. 25 1999.
- [10] T. A. Mutch, W. R. Patterson, A. B. Binder, F. O. Huck, G. R. Taylor, E. C. Levinthal, S. Liebes, Jr., E. C. Morris, J. B. Pollack, and C. Sagan. The surface of Mars - The view from the Viking 1 lander. *Science*, 193:791–801, Aug. 1976.
- [11] R. Reid, P. Smith, M. Lemmon, R. Tanner, M. Burkland, E. Wegryn, J. Weinberg, R. Marcialis, D. Britt, N. Thomas, R. Kramm, A. Dummel, D. Crowe, B. Bos, J. Bell, P. Rueffer, F. Gliem, J. Johnson, J. Maki, K. Herkenhoff, and R. Singer. Imager for Mars Pathfinder (IMP) image calibration. *Journal of Geophysical Research-Planets*, 104(E4):8907–8925, Apr. 25 1999.
- [12] The International Electrotechnical Commission (IEC). *Project Team 61966: Colour Measurement and Management in Multimedia Systems and Equipment - Part 9: Digital Cameras*, volume 100/PT61966(PL)34 of *IEC/4WD 61966-2-1: Part 2-1: Default RGB Colour Space -sRGB*. IEC, Vienna, 1999.
- [13] N. Thomas, W. Markiewicz, R. Sablotny, M. Wutke, H. Keller, J. Johnson, R. Reid, and P. Smith. The color of the Martian sky and its influence on the illumination of the Martian surface. *Journal of Geophysical Research-Planets*, 104(E4):8795–8808, Apr. 25 1999.